

See discussions, stats, and author profiles for this publication at: <https://www.researchgate.net/publication/7971127>

Structure–Function Relationship of Avian Eggshell Matrix Proteins: A Comparative Study of Two Major Eggshell Matrix Proteins, Ansocalcin and OC-17

ARTICLE in BIOMACROMOLECULES · MARCH 2005

Impact Factor: 5.75 · DOI: 10.1021/bm049423+ · Source: PubMed

CITATIONS

32

READS

42

4 AUTHORS, INCLUDING:



Rajamani Lakshminarayanan

Singapore Eye Research Institute

72 PUBLICATIONS 1,108 CITATIONS

SEE PROFILE



Suresh Valiyaveetil

National University of Singapore

232 PUBLICATIONS 6,673 CITATIONS

SEE PROFILE

Structure–Function Relationship of Avian Eggshell Matrix Proteins: A Comparative Study of Two Major Eggshell Matrix Proteins, Ansocalcin and OC-17

Rajamani Lakshminarayanan,[†] Jeremiah S. Joseph,[‡] R. Manjunatha Kini,[‡] and Suresh Valiyaveetil^{*,†}

Department of Chemistry, National University of Singapore, 3 Science Drive 3, Singapore 117543

Received September 15, 2004; Revised Manuscript Received November 10, 2004

The role of individual matrix proteins in avian eggshell calcification is poorly understood despite numerous attempts to characterize and localize their presence in the eggshell matrix. Ansocalcin, the major matrix protein from goose eggshell, was found to induce the formation of calcite crystal aggregates under in vitro. Owing to its high similarity with the chicken eggshell matrix protein ovocleidin 17 (OC-17), a comparative investigation has been carried out to understand the structure–function relationship. RP-HPLC shows that ansocalcin is the major component in extracts of goose eggshells before and after bleach treatment. However, OC-17 was observed in minute quantities in the extract of bleach-treated chicken eggshells. In vitro crystal growth experiments showed that OC-17 and ansocalcin interact differently with the calcite crystals formed. Circular dichroism, intrinsic tryptophan fluorescence, and dynamic light scattering studies showed that, under the conditions used in our experiments, OC-17 does not aggregate in solution or induce the nucleation of calcite aggregates in the concentration range used. These observations indicate that OC-17 and ansocalcin play different roles in the eggshell calcification. To our knowledge, this is the first report on the comparison of properties of homologous eggshell proteins that belong to the same phylogeny.

Introduction

Biomineralization offers organisms the capability to produce inorganic materials with robust shape and morphology for their survival in dynamic environmental conditions. Calcified tissues account for more than 50% of the hard tissues generated.¹ An array of acidic biomacromolecules, such as proteins and proteoglycans, aid the biomineralization process, which is rapid in some cases (e.g., avian eggshells) or a slow process in other cases, occurring over a few years (e.g., bones, teeth, seashells, etc.).² Numerous attempts have been made to understand the molecular mechanisms of biomineralization through isolation and characterization of the soluble organic matrixes (SOM) from various mineralized tissues.³ In a few cases, the major protein component has been purified and sequenced.⁴

Avian eggshell calcification represents a unique model for biomineralization owing to its rapid formation (17–22 h).^{2g} The eggshell fabrication takes place in an extracellular milieu with the help of the macromolecules present/secreted by the oviduct cells as the egg moves along the oviduct.⁵ The resultant calcified shell exhibits a high degree of textural gradient. A number of proteins and proteoglycans have been identified in the chicken eggshell matrix.⁶ Of the three groups of proteins identified in the chicken eggshell matrix, only a few proteins have been tested in vitro to investigate their mineralization capabilities.⁷

Ansocalcin, OC-17, struthiocalcin-1 (SCA-1), and struthiocalcin-2 (SCA-2) are the eggshell-specific proteins extracted from avian eggshells and sequenced completely. SCA-1 shows high identity (65%) and the same number of amino acid residues as ansocalcin, whereas SCA-2 possesses same number of amino acid residues as OC-17 and two phosphoserines located in the same region as OC-17. These proteins belong to the C-type lectin superfamily, yet lack consensus QPD motif that is required for carbohydrate binding.⁸ Recently, the occurrence of two different families of C-type lectins has been demonstrated in other materials.^{8c} Thus, ansocalcin and OC-17 belong to different group of C-type lectin-like proteins.

The traditional bioinformatic approach based on sequence similarity is the first step in inferring the structure–function relationships. It is known that homologous proteins share a common three-dimensional folding and secondary structure, although they may or may not have the same function.⁹ Given the high similarity between ansocalcin and OC-17 (Figure 1), it would be interesting to compare their activity toward the nucleation of calcium carbonate crystals. Therefore, a comparative study on the structure–property relationship of the two eggshell proteins has been carried out and described in detail.

Immunochemically, OC-17 has been observed predominantly in the mamillary bodies and distributed throughout the palisade layer of the eggshell.¹⁰ It is understood that bleach treatment removes the shell membrane and the proteins attached externally to the eggshell. Hence, our first aim was to identify the presence of ansocalcin and OC-17

* To whom correspondence should be addressed. Tel.: (65)68744327. Fax: (65)67791691. E-mail: chmsv@nus.edu.sg.

[†] Department of Chemistry, National University of Singapore.

[‡] Department of Biological Sciences, National University of Singapore.

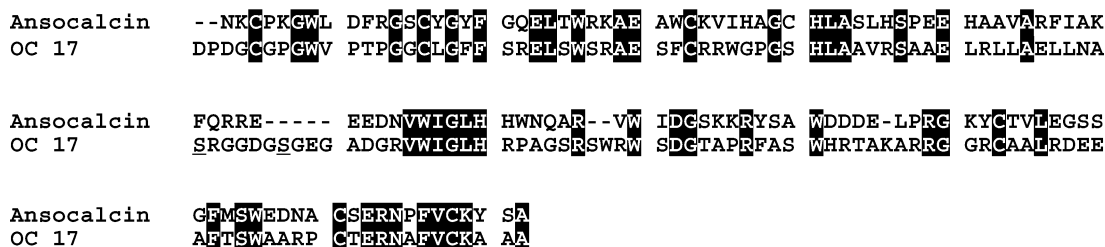


Figure 1. Alignment of the amino acid sequences of ansocalcin and OC-17. The two phosphoserines of OC-17 (S61 and S67) are underlined. The identical amino acid residues are shaded in black.

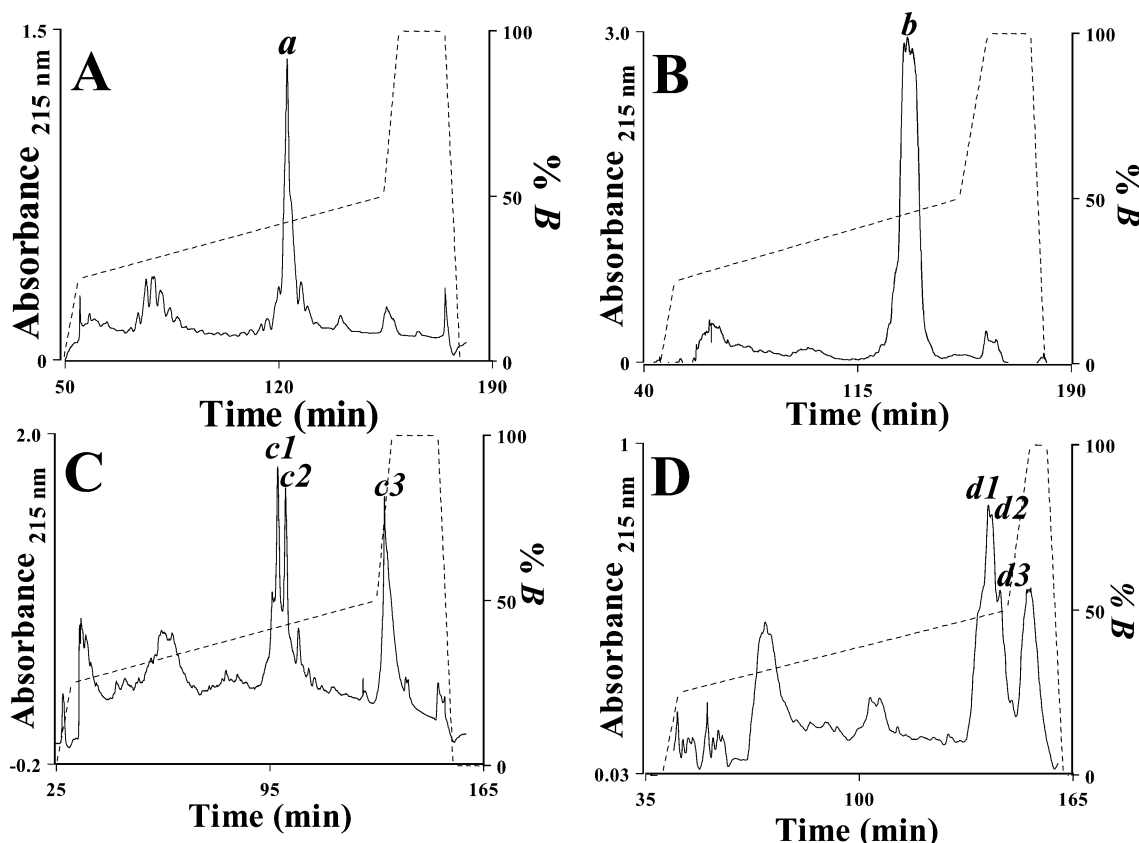


Figure 2. RP-HPLC of the whole eggshell and bleach-treated extracts of the avian eggshells. A and B are the elution profiles of the whole eggshell and bleach-treated eggshell extracts obtained from goose eggshells, whereas C and D are the elution profiles of the extract from the whole eggshells and bleach-treated chicken eggshell, respectively. The fractions pooled for the analysis are represented with italic letters in the figure. The buffer **B** used was 0.1% TFA in 80% acetonitrile.

in whole eggshell extract and extract from bleach-treated eggshells. In vitro crystal growth experiments were carried out to understand the interactions of the two proteins in CaCO_3 crystal nucleation followed by the investigation of the structure of the proteins in solution using CD, fluorescence emission, and DLS studies. Since homologous proteins that share a high identity (>30%) adopt similar folding, a homology modeling of ansocalcin was performed based on the crystal structure of OC-17 to compare the folding pattern in a three-dimensional context.¹¹ From these results, we propose probable roles of the two proteins in the eggshell calcification processes.

Experimental Procedures

Extraction of Ansocalcin and OC-17. Commercially available fresh eggshells were broken and thoroughly washed with Millipore water. They were powdered, bleached briefly

(15–20 min) in sodium hypochlorite solution (5%), washed 5–6 times with Millipore water to remove any residual bleach, and dried overnight at room temperature. Bleached and unbleached eggshells were decalcified separately with 1 N HCl for 30 min, filtered, and centrifuged. The supernatant solution was desalted with an Amicon microconcentrator (YCO5 membrane, 500 MW cutoff) at 4 °C. The turbid solution was centrifuged at 4000 g for 15 min, and the supernatant was removed for fractionation by RP-HPLC.

Protein Purification. The proteins were fractionated on a Jupiter C18 reversed-phase column (5 μm , 250 mm \times 10 mm) using a Vision Workstation (Perkin-Elmer PerSeptive Biosystems). The column was equilibrated with 0.1% trifluoroacetic acid, and a linear gradient of acetonitrile was used for elution. The microconcentrated sample (~15 mg of protein) was injected onto the column and was eluted at a flow rate of 2 mL/min. The elution of the proteins was monitored at a wavelength of 215 and 280 nm.

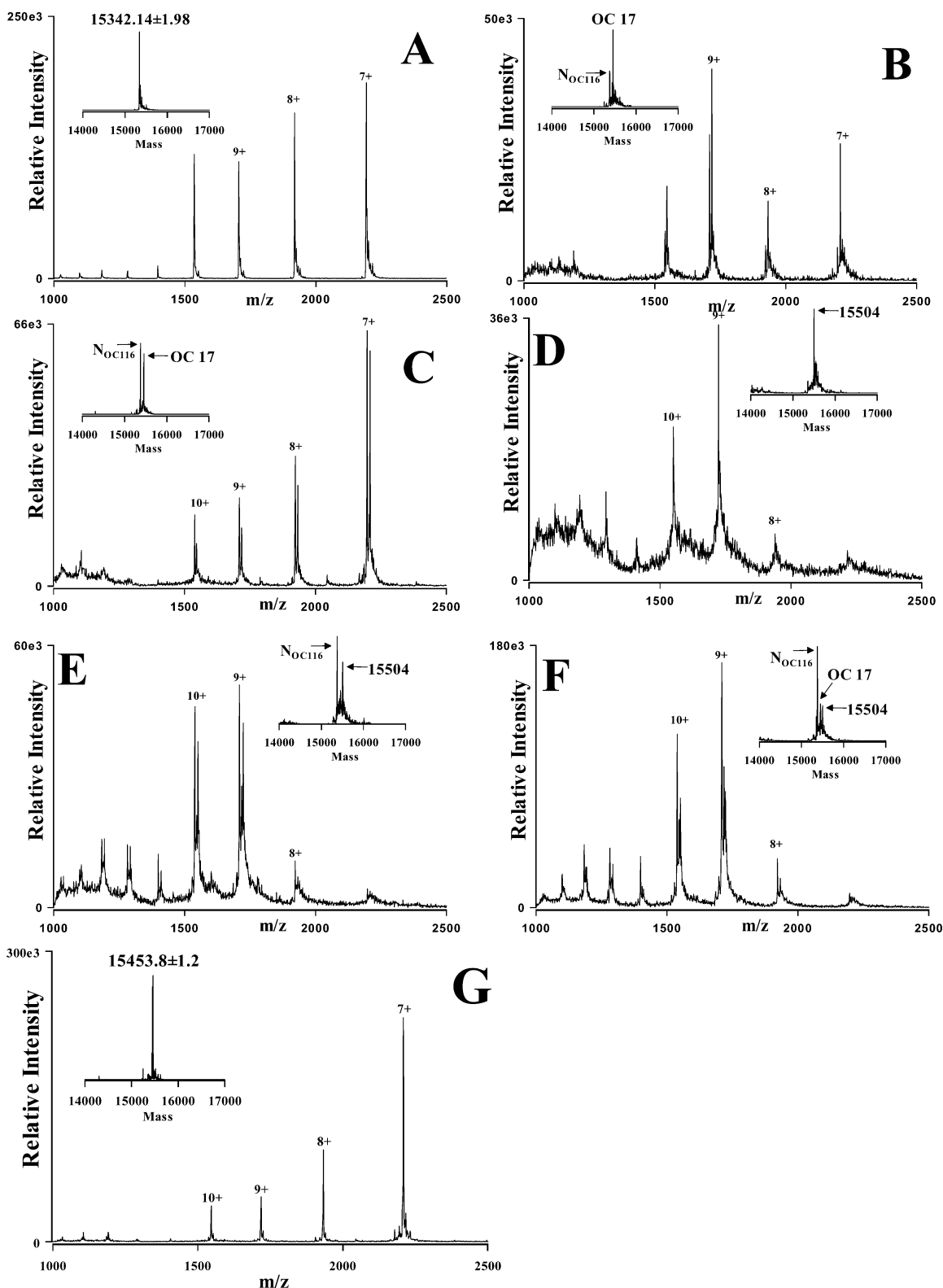


Figure 3. ESI-MS of the various fractions/proteins from whole eggshell and bleach-treated eggshell extracts of the goose and chicken. (A) Ansoalcin from bleach-treated eggshell extract; (B) Fraction c1; (C) Fraction c2; (D) Fraction d1; (E) Fraction d2; (F) Fraction d3; (G) OC-17.

Electrosprayionization Mass Spectrometry. Precise masses of the proteins and peptides were determined by ESI-MS using a Perkin-Elmer Sciex API 300 triple quadrupole instrument equipped with an ion spray interface. The ion spray voltage was set at 4.6 kV and the orifice voltage at 30 V. Nitrogen was used as a curtain gas with a flow rate of

0.6 L/min, whereas compressed air was utilized as the nebulizer gas. The sample was injected into the mass spectrometer at a flow rate of 50 L/min and scanned from mass to charge (m/z) ratio of 500–3000. The multiply charged spectrum was deconvoluted into the mass scale using the Biospec Reconstruct software supplied with an instrument data system.

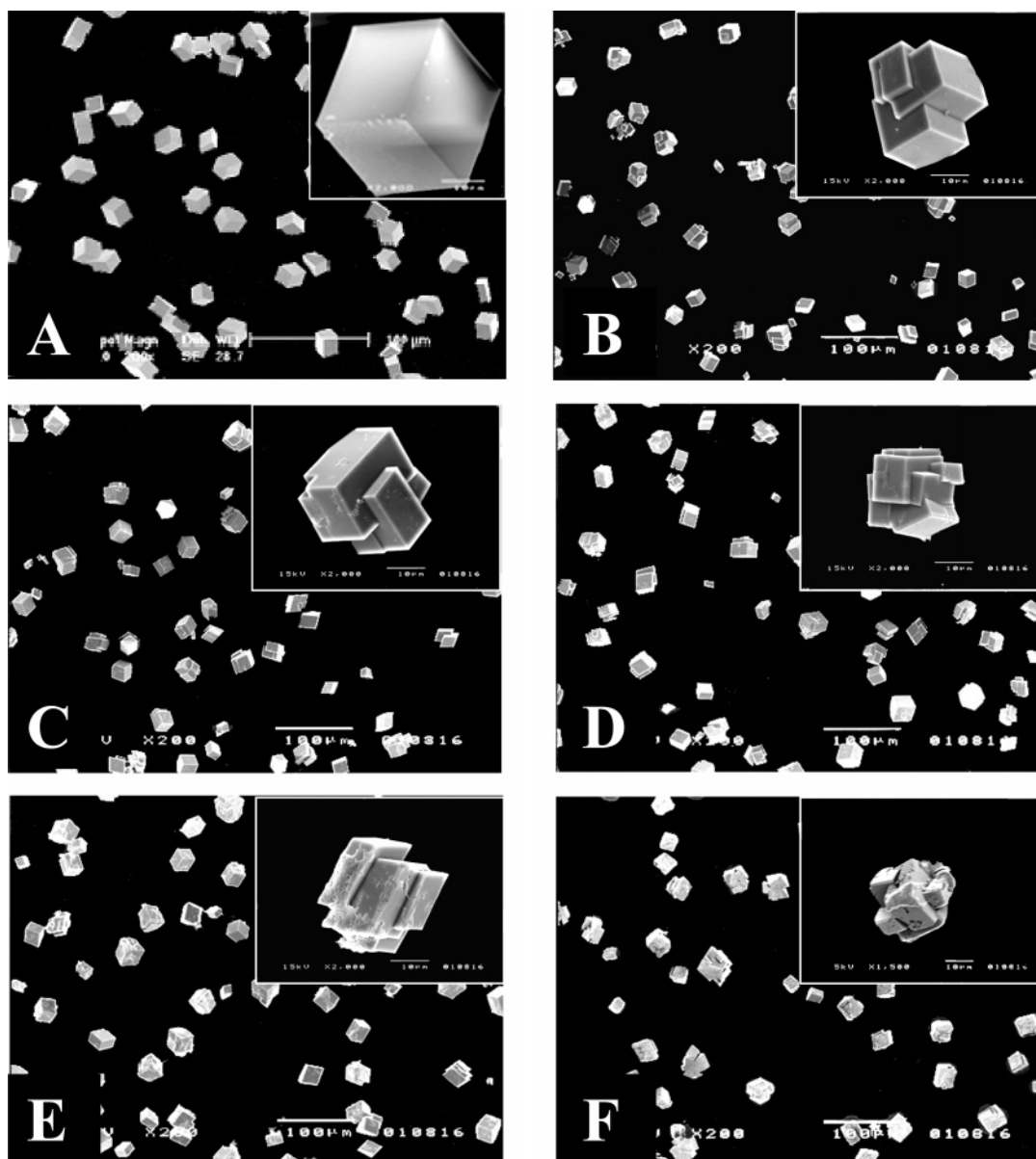


Figure 4. Interaction of OC-17 with the CaCO_3 crystals at various concentrations: (A) control (0 $\mu\text{g/mL}$); (B) 10 $\mu\text{g/mL}$; (C) 50 $\mu\text{g/mL}$; (D) 100 $\mu\text{g/mL}$; (E) 250 $\mu\text{g/mL}$; (F) 500 $\mu\text{g/mL}$. Scale bar = 100 μm .

Crystal Growth Experiments. Calcium carbonate crystals were grown on glass cover slips placed in a calcium chloride solution in a Nunc dish (4×6 wells). Typically, 1 mL of 7.5 mM calcium chloride solution was introduced into the wells containing the cover slips, and the whole setup was covered with aluminum foil with a few pinholes in the top. To study the role of proteins in the calcium carbonate crystallization, aliquots of protein dissolved in 7.5 mM calcium chloride solution at a concentration range of 10–500 $\mu\text{g/mL}$ were introduced into the crystallization wells containing the glass cover slips. Crystals were grown inside a closed desiccator via slow diffusion of CO_2 gases released by the decomposition of solid ammonium carbonate placed at the bottom of the desiccator. After 2 days, the glass slides were carefully lifted from the crystallization wells, rinsed gently with water, air-dried at room temperature, and used for characterization.

Scanning Electron Microscopy. SEM studies on the calcium carbonate crystals were carried out using a JEOL

2200 scanning electron microscope at 15/20 kV after coating with gold to increase the conductivity.

Amino Terminal Sequencing. Amino terminal sequencing of the native proteins was performed by automated Edman degradation using a Perkin-Elmer Applied Biosystems 494 pulsed-liquid-phase protein sequencer (Procise) with an online 785A PTH-amino acid analyzer.

Circular Dichroism Experiments. The secondary structure of the proteins was analyzed using a Jasco J700 circular dichroism spectropolarimeter. The instrument was calibrated with 0.05% (+)-10-camphor sulfonic acid solution. The CD spectra of the protein at a concentration range of 10–500 $\mu\text{g/mL}$ in water were collected using a 0.1-cm sample cell. To study the effect of Ca^{2+} ions, spectra were also recorded in 7.5 mM calcium chloride solution. The instrument optics were flushed with 30 L/min nitrogen gas. A total of three scans were recorded and averaged for each spectrum and baseline subtracted.

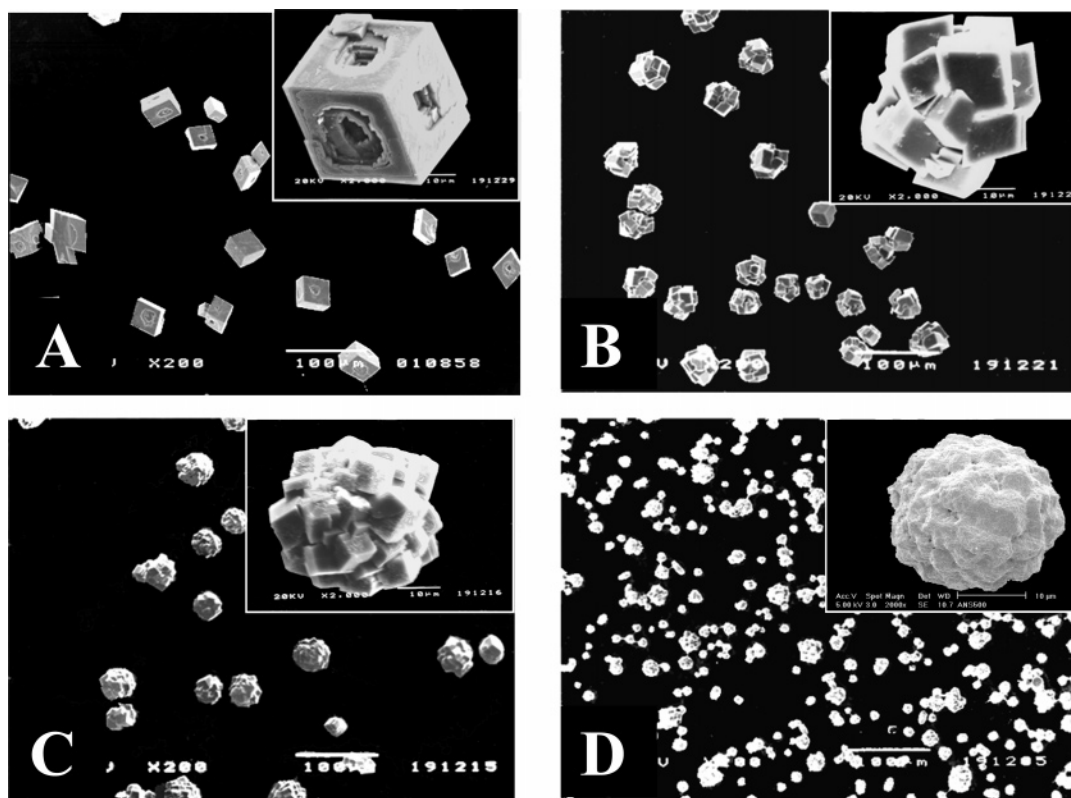


Figure 5. Interaction of ansocalcin with the CaCO_3 crystals. (A) 10 $\mu\text{g/mL}$; (B) 50 $\mu\text{g/mL}$; (C) 100 $\mu\text{g/mL}$; (D) 500 $\mu\text{g/mL}$. Scale bar = 100 μm .

Fluorescence Spectroscopy. The fluorescence emission spectra were collected on a Shimadzu RF-5301PC spectrofluorometer with the emission and excitation band-passes set at 3 nm. The excitation wavelength was set at 295 nm (to selectively excite tryptophan residues), and the spectra were recorded from 300 to 400 nm. Spectra of the proteins were recorded in 7.5 mM calcium chloride solution and in water.

Dynamic Light Scattering Studies. The DLS studies were carried out with a 5-watt argon ion laser (Brookhaven Instruments) and BI-2000SM goniometer coupled to a real time correlator RTG of 12 channels. The power of the laser was varied from 50 to 500 mW depending upon the protein concentration. The data were collected at a scattering angle of 90° to the incident laser beam with a supplying time of 0.8 s. Required amount of proteins were dissolved in water or 7.5 mM calcium chloride solution and studied.

Molecular Modeling. To examine the amino acid sequence of ansocalcin in a three-dimensional context, a molecular model was constructed based on the crystal structure of OC-17 (1GZ2, 1.5 Å resolution). The model was built using the molecular modeling software Xlook (MSI Technologies, San Diego, CA) running on a R10000 workstation (SGI, Mountain View, CA). Using the Biopolymer module of Xlook II, residues of the OC-17 were manually replaced with residues of ansocalcin. The structural parameters were optimized with CVFF-force field in terms of internal energies in order to monitor each step. An initial energy minimization was carried out with the conjugate gradient algorithm down to a maximum derivative of 0.001 Kcal/Å. The freeware WebLab Viewer (Molecular Simulations Inc.) was used for subsequent visualization and annotation of all structures.

Results

Identification of Ansocalcin and OC-17 in the Extracts of Whole Eggshells and Bleach-Treated Eggshells. In a number of calcite exoskeletons, the mechanical strength and the textural properties can be modified by the intracrystalline proteins. These proteins are believed to be involved in the mineralization and therefore become entrapped inside the crystalline matrix.¹² Here, we report a comparative study of the structure and functions of ansocalcin and OC-17 extracted from whole eggshells and bleach-treated eggshells. Figure 2 shows the RP-HPLC of various fractions of the whole eggshell (Figure 2A) and bleach-treated (Figure 2B) goose eggshell extracts. The elution position of ansocalcin is indicated as *a* in the Figure 2A. Ansocalcin elutes along with a 16-kDa protein in the whole eggshell extract as reported earlier.^{8a} However, in the bleach-treated extract, only ansocalcin was found (Figure 2B, Figure 3A) and thus circumvents an additional step involved in the purification.

The RP-HPLC profiles of extracts of whole (Figure 2C) and bleach-treated (Figure 2D) chicken eggshells are shown for comparison. ESI-MS of fraction *cI* is shown in Figure 3B. Deconvolution of the multiply charged spectrum yielded two components of mass $15\,453.8 \pm 1.2$ and $15\,376 \pm 0.64$. The amino terminal sequence of the major component (native protein) unambiguously yielded 26 amino acids **DPDGXG-PGWV PTPGGXLGFF SRELSW** and was confirmed as OC-17 based on the molecular mass and the partial amino acid sequence.¹³ The amino terminal sequence of the minor component was found to be **TPVSLPARAR GNXPQHQIL LKGXNTKHG**. This sequence corresponds to the amino terminus of the proteoglycan core protein OC-116

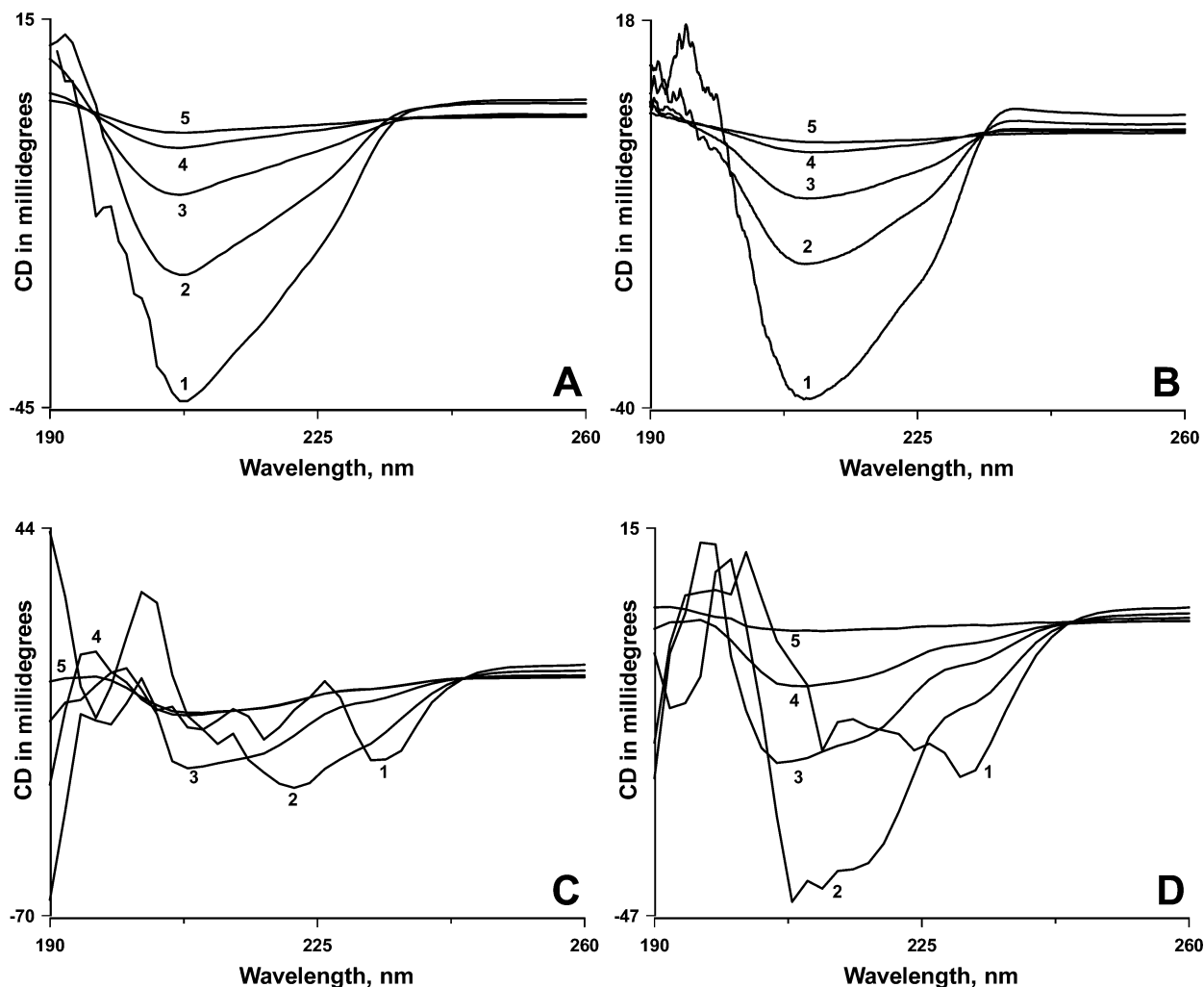


Figure 6. CD spectra of OC-17 and ansocalcin. (A) OC-17 in water; (B) OC-17 in CaCl_2 ; (C) ansocalcin in water; (D) ansocalcin in CaCl_2 . The concentrations used were 500 $\mu\text{g/mL}$ (1); 250 $\mu\text{g/mL}$ (2); 100 $\mu\text{g/mL}$ (3); 50 $\mu\text{g/mL}$ (4); 10 $\mu\text{g/mL}$ (5).

after removal of the putative signal peptide (represented as N_{OC116}) and thus is a degraded fragment of OC-116.¹⁴ This fragment has a larger mass than that reported earlier, which may be due to different methods of extraction of the matrix components employed in various labs.¹⁵ Fraction *c2* was found to contain equal amount of N_{OC116} and OC-17 (Figure 3C). ESI-MS of fraction *d1* of the bleach-treated eggshell extract showed a mass of 15504 (Figure 3D) whereas fraction *d2* contained N_{OC116} and a 15504 Da protein (Figure 3E). However, fraction *d3* showed three components: N_{OC116} , OC-17 and a 15504 Da protein (Figure 3F). These results showed that (a) ansocalcin is the major component in extracts of both whole and bleach-treated goose eggshells and (b) OC-17 is the major component in whole chicken eggshell extract and less abundant in the bleach-treated eggshell extract.

Interaction of Ansocalcin and OC-17 with CaCO_3 Crystals. To compare the properties of OC-17 and ansocalcin, OC-17 was purified extensively from the whole chicken eggshell extract, and the homogeneity was confirmed by ESI-MS and N-terminal sequencing (Figure 3G). The homogeneous fraction was lyophilized and used in our experiments. Figures 4 and 5 show the changes in CaCO_3 growth pattern in the presence of OC-17 and ansocalcin. The features of the calcite crystal growth pattern are different in the presence

of OC-17 and ansocalcin. At low levels of OC-17 (10–100 $\mu\text{g/mL}$, Figure 4B–D), the crystals were twinned and less-aggregated. The corners of the twinned crystals were curved at 250 $\mu\text{g/mL}$ (Figure 4E). At the highest concentration of OC-17 (500 $\mu\text{g/mL}$), the corners of the crystals appeared to be smooth (Figure 4F). The results obtained in our in vitro crystallization experiments appeared to differ from the results reported recently using OC-17, which may be due to the high salt concentration in their experiments.^{11d} However, in the presence of ansocalcin, two distinct effects were observed. At lower concentrations (up to 10 $\mu\text{g/mL}$, Figure 5A), crystals with screw dislocations along the $\{10\cdot4\}$ faces were formed, and at high concentrations (>50 $\mu\text{g/mL}$), polycrystalline calcite aggregates were nucleated (Figure 5B). The spherical aggregates formed at 50 and 100 $\mu\text{g/mL}$ encompassed perfect rhombohedral crystallites (Figure 5C). The shape of the aggregates was disturbed as the ansocalcin concentration was increased to 250 $\mu\text{g/mL}$. The aggregates formed at this level exhibited various shapes, such as spherical, ellipsoidal, etc., with concomitant reduction in the overall size. Further reduction in size and appearance of microscopic pores were the characteristics of the aggregates formed at 500 $\mu\text{g/mL}$ ansocalcin (Figure 5D). The number of crystals per unit area (nucleation density) is markedly

increased as the concentration of ansocalcin was increased from 100 to 500 $\mu\text{g/mL}$. Thus, despite sharing a high similarity, OC-17 and ansocalcin interacted differently with calcite crystals.

CD and Intrinsic Tryptophan Fluorescence Studies.

Since ansocalcin and OC-17 showed differences in their ability to interact with calcite crystals, the conformations of the proteins were investigated using CD and fluorescence emission studies. Figure 6 compares the concentration- and calcium-dependent changes in the secondary structure of ansocalcin and OC-17. For OC-17 in water (Figure 6A), the appearance of a negative minimum at 207 nm and positive maximum at 194 nm were characteristics of a high degree of α -helix conformation. Appearance of a shoulder around 196 nm at 500 $\mu\text{g/mL}$ is indicative of the presence of a small amount of unordered structure in OC-17. The dichroic minimum is shifted to 209 nm in the presence of calcium ions indicating slight changes in the secondary structure, presumably due to calcium binding (Figure 6B). On the other hand, ansocalcin exhibited a complex pattern with change in concentration of the protein (Figure 6, parts C and D). At lower concentrations, the appearance of dichroic minima at 207 and 218 nm is indicative of the presence of α -helix and β -sheet conformations. The dichroic minimum was shifted to 230 nm at higher concentration in water and in CaCl_2 indicating significant changes in the secondary conformation. These changes were attributed to the existence of monomer-multimer equilibrium present in the ansocalcin solution. Thus, the CD studies indicated that the secondary structure of OC-17 is independent of concentration and calcium ions, whereas the secondary structure changes strongly with the concentration of ansocalcin.

Of the eight tryptophans in ansocalcin and OC-17, six are conserved; however, their emission characteristics seem to be different (Figure 7). Ansocalcin had an emission maximum at 346 nm, whereas it was slightly blue-shifted to 341 nm for OC-17 indicating the partially buried nature of the fluorophores. To study the effect of protein concentration, we recorded the emission spectra at different concentrations of the proteins and plotted the change in intensity of emission maxima (F_{max}) with concentration (Figure 7C). For OC-17, the F_{max} increases progressively up to 500 $\mu\text{g/mL}$ and decreased slightly at 1 mg/mL, whereas the F_{max} reached a maximum at 250 $\mu\text{g/mL}$ for ansocalcin and decreased at higher concentrations. Thus, at higher concentrations, both proteins quench the emission from tryptophan residues, although the concentration required for quenching is different for ansocalcin and OC-17. In addition, the magnitude of quenching is greater in the case of ansocalcin than for OC-17. A similar effect was observed when the emission spectrum was monitored in water (data not shown).

Dynamic Light Scattering Studies. To obtain a better insight into the solution behavior of ansocalcin, DLS experiments were carried out. This technique has the advantage of rapid analysis of aggregation properties without perturbing the system. Experiments were performed both in water and in the presence of 7.5 mM calcium chloride solution. For OC-17 at a concentration of 3 mg/mL, particles

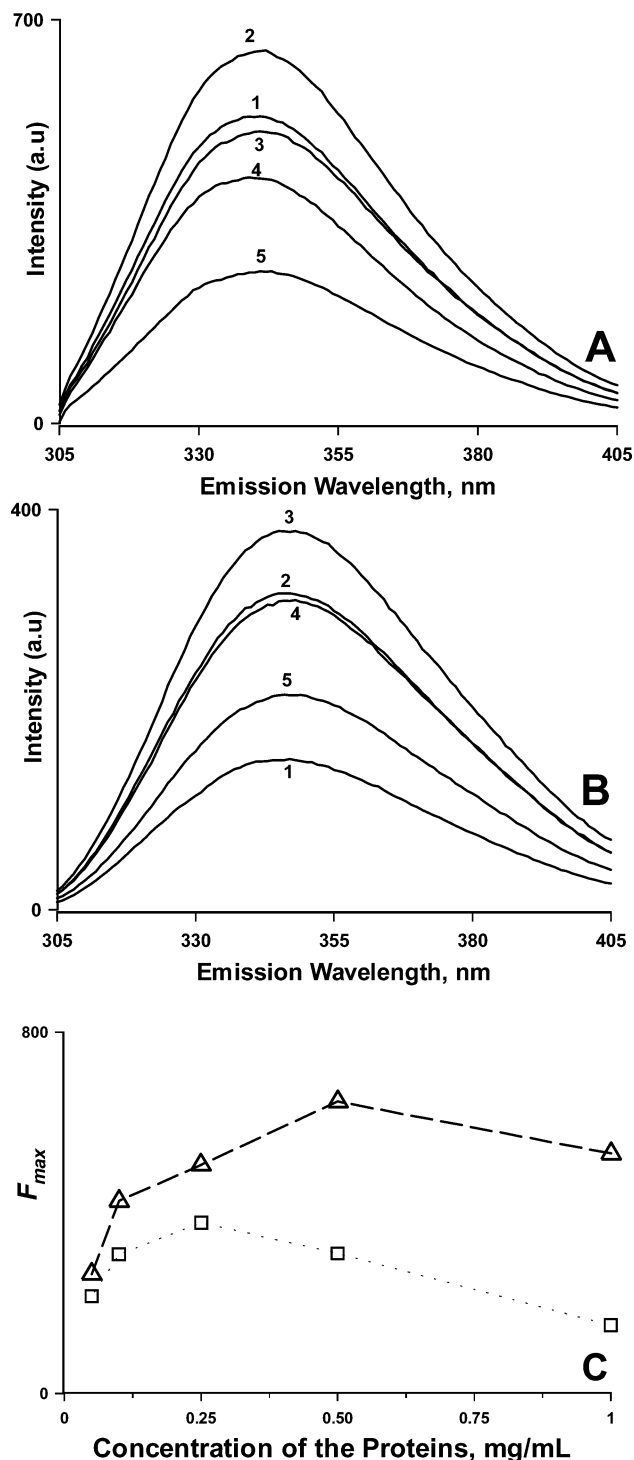


Figure 7. Intrinsic tryptophan fluorescence of OC-17 and ansocalcin in CaCl_2 solution. (A) Emission spectra of OC-17; (B) Emission spectra of ansocalcin. The concentrations used were 1000 $\mu\text{g/mL}$ (1); 500 $\mu\text{g/mL}$ (2); 250 $\mu\text{g/mL}$ (3); 100 $\mu\text{g/mL}$ (4); 50 $\mu\text{g/mL}$ (5). (C) Plot of intensity of emission maxima with increase in concentration of OC-17 (broken line with triangles) and ansocalcin (dotted line with squares). The emission maxima is expressed as F_{max} .

of mean hydrodynamic diameter 10.54 nm were observed and remained the same even after dilution (Figure 8, parts A and B). Addition of Ca^{2+} seems to alter the size distribution slightly. However, for ansocalcin under all conditions, species of various populations, whose size is indicated by hydrodynamic diameter, coexist in solution (Figure 8D–F). At 3 mg/mL in water, aggregates with 83.4

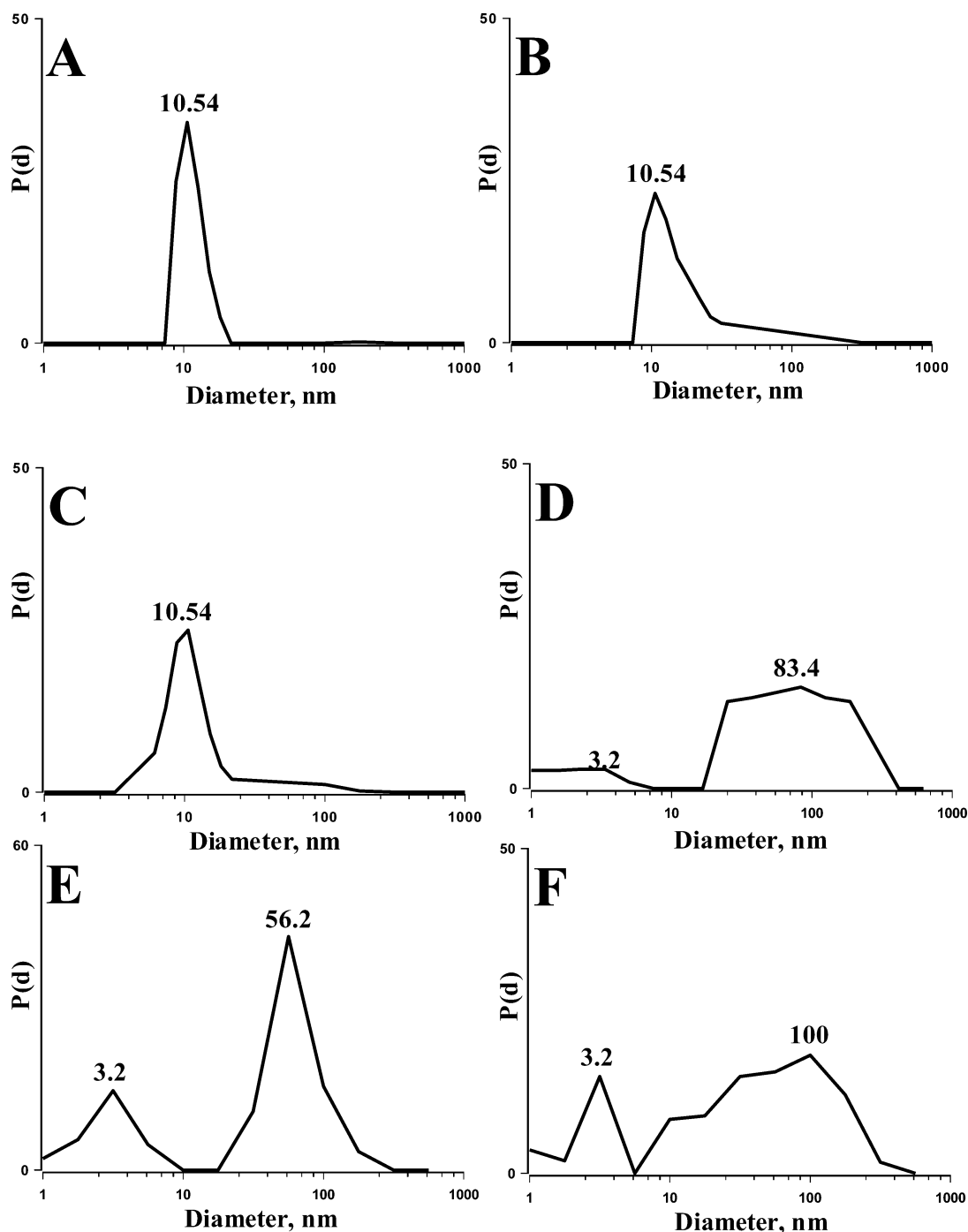


Figure 8. Dynamic light scattering measurements of OC-17 at 3 mg/mL in water (A), 1.5 mg/mL in water (B), 3 mg/mL in 7.5 mM CaCl_2 solution (C) and ansocalcin at 3 mg/mL in water (D), 1.5 mg/mL in water (E) and 3 mg/mL in 7.5 mM CaCl_2 solution (F).

nm size were observed (Figure 8D). Upon dilution, the size was reduced to 56.2 nm and the population of monomeric species increased (Figure 8E). When the DLS measurement was carried out in the presence of Ca^{2+} , for ansocalcin, the size distribution was broadened compared to that in water presumably due to calcium capping suggesting that the aggregation was not significantly affected by the presence of Ca^{2+} ions (Figure 8F). These results indicated ansocalcin exist in the aggregated form whereas OC-17 does not aggregate at the concentrations used in our experiments.

Molecular Modeling Studies. The crystal structure of OC-17 and the molecular model of ansocalcin possess folding

patterns that are somewhat similar to human lithostathine protein.¹⁶ The noticeable differences include the following: ansocalcin and OC-17 have two helices and eight β -strands, of which two quartets of them form antiparallel β -sheets. Figure 9 illustrates the sequential connectivity and the topology of amino acids present in ansocalcin and OC-17. In comparing the folding pattern of ansocalcin with OC-17, very little deviation from the template structure was observed owing to their high identity (Figure 10, parts A and C). However, an important difference is the existence of the loop l_6 , which connects $\alpha 2$ and $\beta 4$ is extended over more space in ansocalcin compared to OC-17. This region comprises the acidic and basic multiplets Arg61-Arg62-Glu63-Glu64-

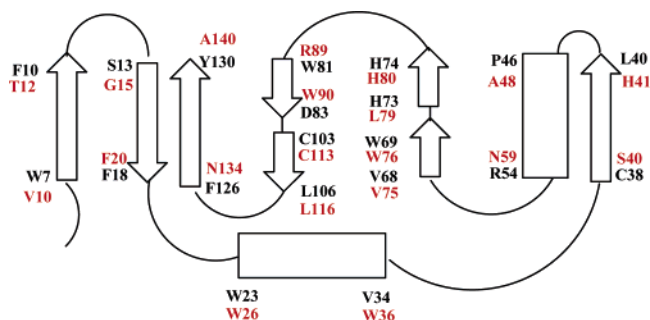


Figure 9. Schematic diagrams of OC-17 and ansocalcin topology. The α -helices are shown as rectangles and the β -strands are depicted in arrows. The amino acid sequence of the OC 17 is represented in red letters, whereas the amino acid sequence of ansocalcin is represented in black letters.

Glu65-Asp66 (indicated by the arrow in Figure 10C). The molecular model of ansocalcin revealed the distribution of charged residue clusters on the surface (Figure 10D). The C-terminus multiplies Asp93-Asp94-Asp95-Asp96 and Glu116-Asp117 and Glu107 form a large cluster, whereas the stretch Glu63-Glu64-Glu65-Asp66 and Glu21 form another cluster. The surface structure of ansocalcin and OC-17 revealed a totally contrasting polarity; the surface of ansocalcin is negatively charged (Figure 10D), whereas OC-17 has a high degree of positive charges on the surface (Figure 10B).

Discussion

Proteins exhibit their activity through a myriad of interactions with various other components present in a particular biological environment. To understand the mechanism of protein-mineral interactions, it is important to study the contribution from individual components that make the final structure. Here we compare the two proteins that not only share a high degree of amino acid identity but also belong to the same phylum (Avia). The following are the important findings of our investigations.

First, ansocalcin is the major component in the extract of the whole and bleach-treated goose eggshells, whereas OC-17 is the major component in the extract of whole chicken eggshells and is present in small amounts in the extract of bleach-treated eggshells. Resistance of the ansocalcin to bleach treatment indicates an intimate association of the protein with the inorganic matrix. The observed high amount of ansocalcin in the extract of bleach-treated goose eggshell indicates that ansocalcin may be active in goose eggshell mineralization. On the other hand, OC-17 is present in smaller amounts in the bleach-treated eggshell extract relative to the whole eggshell extract. It is likely that the large aggregates formed by OC-17 may have little room to enter into the calcite lattice. Such large aggregates may form a proteinacious network on the shell membrane and may be involved in the initial part of eggshell calcification. This is

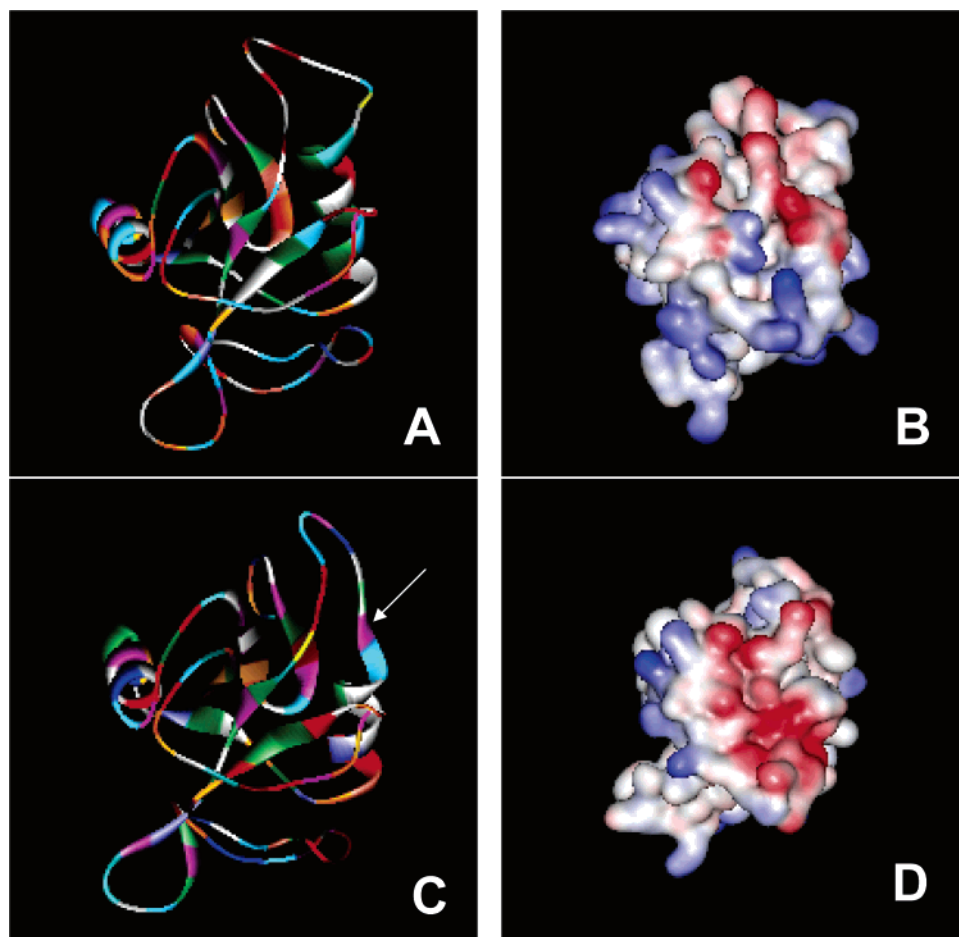


Figure 10. Molecular models of ansocalcin. (A) Crystal structure of OC-17 (C) Molecular model of ansocalcin derived from OC-17 crystal structure. The individual amino acid residues are colored in the figure. (B) and (D) indicates the surface polarity of OC-17 and ansocalcin, respectively. The acidic surfaces are colored in red while the basic surfaces are colored in blue.

clearly evident in the *in vitro* crystallization experiments, since OC-17 has little influence morphology of calcite crystals while ansocalcin induced the formation of polycrystalline calcite crystal aggregates. In addition to this, the nucleation density is significantly increased at a higher concentration of ansocalcin.

Second, the conformation of ansocalcin changed significantly as a function of concentration of the protein, whereas no significant changes were observed for OC-17 as indicated by CD and intrinsic tryptophan fluorescence studies. The presence of excessive scattering in the CD spectra and concentration-dependent quenching of the tryptophan fluorophores indicated the existence of an aggregated state for ansocalcin. However, for OC-17, there was no significant change in the secondary structure with an increase in concentration suggesting that it exists predominantly in the nonaggregated state at these levels. The presence of multiplets of acidic and basic amino acids in the vicinity may be responsible for the relatively “exposed” nature of the tryptophan fluorophores in ansocalcin compared to OC-17. The emission spectra further showed that the “exposed” nature of tryptophan residues is unaltered even in the aggregated state (indicated by the absence of any blue shift in the emission spectrum at higher concentration). It is interesting to note that the magnitude of quenching is less for OC-17, although it has a high amount of arginine (13.4 %), which efficiently quenches tryptophan fluorescence.¹⁷ For ansocalcin, the particle size and size distribution were significantly high with a broad size distribution in the presence of Ca^{2+} ions. Thus, protein aggregation appeared to be responsible for the formation of polycrystalline calcite aggregates and the increase in nucleation density.

Third, when the three-dimensional structures of ansocalcin and OC-17 were compared, a few significant differences were observed in the region where acidic and basic amino acids exist as multiplets. The surface structure of ansocalcin is highly polarized; one side has a high amount of negatively charged amino acids and positively charged amino acids on the other side which exists in clusters. However, in OC-17, a distribution of predominantly positively charged amino acids was observed at the surface.

It is conceivable that the islets of acidic amino acids in ansocalcin interact with the growing calcite crystals thereby inducing spiral pits along the {104} faces. At higher concentration, the motion of these islets is restricted owing to protein aggregation, which reduces the motion of the molecule in solution. Such restricted motion would then allow each islet to act as a nucleating site resulting in the formation of crystal aggregates and an increase in the nucleation density. Phosphoprotein from rat dentin inhibits the crystallization of hydroxyapatite *in vitro* but induces mineral formation when adsorbed onto a solid matrix.¹⁸ The author's explanation of this is that adsorption of the protein restricts its motion and results in an increase in local cation concentration owing to the polyanionic nature of the protein. Hence, it is likely that the negatively charged side chains in ansocalcin act as if they were adsorbed on a solid matrix in the aggregated state, forming crystal aggregates and increasing the crystal nucleation density. Recently, the importance

of such repetitive charged motifs in the nucleation of crystal aggregates has been established using synthetic peptides.¹⁹

Comparing the hydrophathy of ansocalcin and OC-17, amino acid sequences indicated significant differences in the central region (residues 30–100 for ansocalcin). For ansocalcin, this region is characterized by perfect amphiphilic geometry comprising stretches of hydrophobic and hydrophilic amino acids. Such a feature may then assist specific interactions with the mineral phase, which helps the protein to be incorporated into a calcite crystal lattice enabling it to be resistant toward hypochlorite bleaching. The deposition of ansocalcin on crystal aggregates indicates that it organizes and protects small crystallites against feathering during the early stages of crystal growth. Thus, two important roles for ansocalcin in goose eggshell calcification are suggested. As a “template”, ansocalcin induces crystal aggregation, and as a “protein-bridge”, it stabilizes the newly formed crystallites against feathering. The concept of macromolecular bridging was introduced to explain the ability of high molecular weight poly(acrylic acid) to cause aggregation of growing apatite crystals.²⁰ The inability of OC-17 to form crystal aggregates may be due to the absence of multiplets of acidic/basic amino acids or due to the presence of a higher ratio of basic to acidic amino acid residues. It is possible that a high concentration of OC-17 is required to form large aggregates, and the aggregated form may be involved in the initial stage of the eggshell calcification.¹⁰ Since the size of the aggregate is large, the calcite lattice structure may not accommodate it, thereby making it susceptible to oxidation by hypochlorite bleach.

In conclusion, we established that ansocalcin is present in significant amounts in both whole eggshell and bleach-treated goose eggshells and OC-17 is less abundant in the extract from bleach-treated chicken eggshells. These two proteins belong to the C-type lectin family and share a high degree of similarity. But they interact differently with the growing calcium carbonate crystals suggesting that their role in eggshell calcification is different. The conformation of ansocalcin changes in a concentration-dependent manner, whereas the conformation of OC-17 is unaffected with concentration, which indicates more intermolecular interactions take place in ansocalcin than OC-17. Based on the molecular modeling results, we suggest that the stretches of acidic and basic amino acids present in ansocalcin play a significant role in the nucleation and growth of calcite crystals. We believe that the results presented here may shed some light on the role played by the individual proteins in avian eggshell mineralization.

Acknowledgment. The authors thank the technical staffs of the Protein & Proteomics Centre, Department of Chemistry, and Department of Biological Sciences, NUS, for their help. R.L.N. thanks the Singapore Millennium Foundation for the award of fellowship.

References and Notes

- (1) Lowenstam, H. A. *Science* **1981**, *211*, 1126–1131.
- (2) (a) Shen, X. Y.; Belcher, A. M.; Hansma, P. K.; Stucky, G. D.; Morse, D. E. *J. Biol. Chem.* **1997**, *272*, 32472–32481. (b) Aizenberg, J.; Lambert, G.; Weiner, S.; Addadi, L. *J. Am. Chem. Soc.* **2002**, *124*, 32–38. (c) Amey, L.; De Becker, G.; Killian, C.; Wilt, F.; Kemps,

- R.; Kuypers, S.; Dubois, P. *J. Struct. Biol.* **2001**, *134*, 56–66. (d) Wilt, F. H. *J. Struct. Biol.* **1999**, *126*, 216–226. (e) Wang, R. Z.; Addadi, L.; Weiner, S. *Philos. Trans. R. Soc. London B* **1997**, *352*, 469–480. (f) Addadi, L.; Weiner, S. *Angew. Chem. Int. Ed. Eng.* **1992**, *31*, 153–169. (g) Kuhn, L. T.; Fink, D. J.; Heuer, A. H. *Biomimetic Materials Chemistry*; Mann, S., Ed.; VCH Publishers: New York, 1996; pp 41–68.
- (3) (a) Choi, C. S.; Kim, Y. W. *Biomaterials* **2000**, *21*, 213–222. (b) Bouropoulos, N.; Weiner, S.; Addadi, L. *Chem.—Eur. J.* **2001**, *7*, 1881–1888. (c) Weiner, S.; Addadi, L. *Trends Biochem. Sci.* **1991**, *16*, 252–256. (d) Dauphin, Y.; Denis, A. *Comp. Biochem. Physiol. A* **2000**, *126*, 367–377. (e) Dauphin, Y. *J. Biol. Chem.* **2003**, *278*, 15168–15177.
- (4) (a) Miyamoto, H.; Miyashita, T.; Okushima, M.; Nakano, S.; Morita, T.; Matsushiro, A. *Proc. Natl. Acad. Sci.* **1996**, *93*, 9657–9660. (b) Sarashina, I.; Endo, K. *Mar. Biotechnol.* **2001**, *3*, 362–369. (c) Testeniere, O.; Hecker, A.; Le Gurun, S.; Quennedey, B.; Graf, F.; Luquet, G. *Biochem. J.* **2002**, *361*, 327–335. (d) Samata, T.; Hayashi, N.; Kono, M.; Hasegawa, K.; Horita, C.; Akera, S. *FEBS Lett.* **1999**, *462*, 225–229. (e) Mann, K.; Weiss, I. M.; Andre, S.; Gabius, H. J.; Fritz, M. *Eur. J. Biochem.* **2000**, *267*, 5257–5264. (f) Bedouet, L.; Sculler, M. J.; Marin, F.; Milet, C.; Lopez, E.; Giraud, M. *Comp. Biochem. Phys. B* **2001**, *128*, 389–400.
- (5) (a) Arias, J. L.; Fernández, M. S.; Laria, V. J.; Janicki, J.; Heuer, A. H.; Caplan, A. I. *Mater. Res. Soc. Proc.* **1991**, *218*, 193–201. (b) Fernández, M. S.; Moya, A.; Lopez, L.; Arias, J. L. *Matrix Biol.* **2001**, *19*, 793–803.
- (6) (a) Nys, Y.; Hincke, M. T.; Arias, J. L.; Garcia-Ruiz, J. M.; Solomon, S. E. *Poult. Avian Biol. Rev.* **1999**, *10*, 143–166. (b) Nys, Y.; Gautron, J.; McKee, M. D.; Garcia-Ruiz, J. M.; Hincke, M. T. *World Poult. Sci. J.* **2001**, *57*, 401–413.
- (7) (a) Hincke, M. T.; Gautron, J.; Panheleux, M.; Garcia-Ruiz, J.; McKee, M. D.; Nys, Y. *Matrix Biol.* **2000**, *19*, 443–453. (b) Gautron, J.; Hincke, M. T.; Panheleux, M.; Garcia-Ruiz, J. M.; Boldicke, T.; Nys, Y. *Connect. Tissue Res.* **2001**, *42*, 255–267.
- (8) (a) Mann, K.; Siedler, F. *Biochim. Biophys. Acta* **2004**, *1696*, 41–50. (b) Lakshminarayanan, R.; Valiyaveetil, S.; Rao, V. S.; Kini, R. M. *J. Biol. Chem.* **2003**, *278*, 2928–2936. (c) Mann, K. *Brit. Polut. Sci.* **2004**, *45*, 483–490.
- (9) Pearson, W. R. *Methods Enzymol.* **1996**, *266*, 227–258.
- (10) Hincke, M. T.; Tsang, C. P. W.; Courtney, M.; Hill, V.; Narbaitz, R. *Calcif. Tissue Intl.* **1995**, *56*, 578–583.
- (11) (a) Orengo, C. A.; Jones, D. T.; Thornton, J. M. *Nature* **1994**, *372*, 631–634. (b) Creighton, T. E. In *Proteins: Structures and Molecular Properties*, 2nd ed.; W. H. Freeman: New York, 1993. (c) Reyes-Grajeda, J. P.; Juregui-Ziga, D.; Rodriguez-Romero, A.; Hernandez-Santoyo, A.; Bolanos-Garcia, V. M.; Moreno, A. *Prot. Pept. Lett.* **2002**, *9*, 253–260. (d) Reyes-Grajeda, J. P.; Moreno, A.; Romero, A. *J. Biol. Chem.* **2004**, *279*, 40876–40881.
- (12) (a) Berman, A.; Addadi, L.; Kvick, A.; Leiserowitz, L.; Nelson, M.; Weiner, S. *Science* **1990**, *250*, 664–667. (b) Belcher, A. M.; Wu, X. H.; Cristensen, R. J.; Hansma, P. K.; Stucky, G. D.; Morse, D. E. *Nature* **1996**, *381*, 56–57. (c) Aizenberg, J.; Hanson, J.; Ilan, M.; Leiserowitz, L.; Koetzle, T. F.; Addadi, L.; Weiner, S. *FASEB J.* **1995**, *9*, 262–268.
- (13) Mann, K.; Siedler, F. *Biochem. Mol. Biol. Int.* **1999**, *47*, 997–1007.
- (14) Hincke, M. T.; Gautron, J.; Tsang, C. P. W.; McKee, M. D.; Nys, Y. *J. Biol. Chem.* **1999**, *274*, 32915–32923.
- (15) Mann, K.; Hincke, M. T.; Nys, Y. *Matrix Biol.* **2002**, *21*, 383–387.
- (16) Bertrand, J. A.; Pignol, D.; Bernard, J. P.; Verdier, J. M.; Dagorn, J. C.; Fontecilla-Camps, J. C. *EMBO J.* **1996**, *15*, 2678–2684.
- (17) Ruddock, L. W.; Hirst, T. R.; Freedman, R. B. *Biochem. J.* **1996**, *315*, 1001–1005.
- (18) Lussi, A.; Crenshaw, M. A.; Linde, A. *Arch. Oral Biol.* **1988**, *33*, 685–691.
- (19) Ajikumar, P. K.; Lakshminarayanan, R.; Valiyaveetil, S.; Kini, R. M. *Biomacromolecules* **2003**, *4*, 1321–1326.
- (20) Nancollas, G. H.; Budz, J. A. *J. Dent. Res.* **1990**, *69*, 1678–1685.

BM049423+